Large-scale molecular dynamics study of liquid K-Cs alloys: Structural, thermodynamic, and diffusion properties

J.-F. Wax and N. Jakse*
Laboratoire de Physique des Milieux Denses, Université Paul Verlaine-Metz, 1, Boulevard F. D. Arago, CP 87811, 57078 Metz Cedex 3, France

(Received 5 September 2006; revised manuscript received 7 November 2006; published 8 January 2007)

Molecular dynamics simulations are performed to study the evolution of the properties of K-Cs alloys with composition. Interatomic interactions are described by the second-order pseudopotential-perturbation formalism. The validity of this model is ascertained by comparison with available experimental results of total structure. Partial structures are investigated in detail in relation with interaction features. The large size of the simulated box provides an accurate description of the low-q behavior of the partial structure factors, yielding some thermodynamic properties like the isothermal compressibility. Individual and collective dynamic properties are considered through the self-diffusion and interdiffusion coefficients. An analysis of these properties indicates a cancellation between homocoordination and heterocoordination tendencies so that the system behaves nearly like an ideal mixture in the whole range of compositions despite the complex metallic interactions. We emphasize that such a behavior can be understood from a competition between size asymmetry and attraction nonadditivity on one side, and attraction asymmetry on the other side.

DOI: 10.1103/PhysRevB.75.024204 PACS number(s): 61.25.Mv, 61.20.Ja, 66.10.−x, 31.15.Qg

I. INTRODUCTION

The contribution of molecular dynamics (MD) simulations to our understanding of liquid matter has been unparalleled during the last three decades. The description of both static and dynamic structures of pure liquids at the microscopic scale benefited from the numerous simulations performed to date. Simple systems such as Lennard-Jones fluids, or more realistic ones such as noble gas or simple liquid metals where interactions are depicted by effective pair potentials were copiously studied with classical MD. On the other hand, semiconducting liquids or molten transition metals, etc., require a more sophisticated description of the interactions and are the subject of intensive *ab initio* MD computations since about one decade.

By comparison, however, liquid alloys did not arouse a great enthusiasm on both theoretical and experimental points of view. This is mainly due to additional difficulties in the description of mixtures. On the experimental side, the partial functions necessary to describe the structure of a mixture are usually provided by isotopic substitution method in neutron diffraction experiments.[1] This is difficult, expensive and sometimes even impossible to carry out (some elements only exist as a single stable isotope). On the theoretical point of view, the difficulties arise from the description of the interactions. In metallic systems, these are density dependent due to the screening effect of the electron gas. Moreover, the density of an alloy being strongly dependent on the concentration of each species, the influence of the environment is consequently great. So, it is rather delicate to set up a description of the interactions adequate for such a large range of density without using arbitrary parameters. Of course, *ab initio* methods are able to describe correctly the interactions whatever the density, but these methods are extremely time consuming, reducing the size of the simulated systems. Since liquid alloys sometimes exhibit composition fluctuations in a long range, the large simulation box required to study these behaviors prevents from applying *ab initio* methods. Moreover, in the case of dilute mixtures, too small a number of particles implies poor statistics.

This might also explain why systematic studies in the whole concentration range of the microscopic structure of a metallic alloy by MD simulation is still lacking in the literature even if some results have already been presented for given alloys at given compositions of particular interest. So, the evolution of the structural properties with composition is far from being completely understood. Indeed, this evolution may certainly be very different from one alloy to another according to the variety of behaviors that real systems can exhibit, ranging from nonmiscibility to compound forming and passing by homocoordination, random mixing or heterocoordination.

Liquid alloys of alkali metals are systems for which the static structure was studied experimentally. A typical case is K-Cs since its static structure has already been studied by x rays and neutron diffusion.[2,3] As with most of the liquid alloys, only the total structure factor (at four compositions, namely 30, 50, 80, and 85 at. %) including its low-q limit are available. According to its electrical resistivity,[4] the nearly free character of the conduction electrons is established, which means that the effective interactions can be described by means of a second-order pseudopotential perturbation method whatever the composition of the alloy. Considering the phase diagram,[5] K-Cs is a perfectly miscible system that is usually considered as quite an ideal mixture[3] although, strictly speaking, it is not because of the size mismatch of its two components. Such a real system is consequently an interesting purpose for a systematic study of the evolution of structural properties versus composition before extending it to trickier systems. As we will see, this system is in a central place, exhibiting neither homocoordination nor heterocoordination tendencies, what is rather exceptional for a real metallic system. Consequently, it can be considered as a reference for other mixtures to point out some departure from it.

TABLE I. Mean atomic volumes, $\Omega_0 = V/N$, and characteristics of the pair interaction potentials for each alloy studied. Notations are defined in the text.

Alloy	Ω_0 (a.u.)	σ_{11} (a.u.)	ϵ_{11} (10^{-3} a.u.)	$\alpha=\frac{\sigma_{22}}{\sigma_{11}}$	$\beta=\frac{\epsilon_{22}}{\epsilon_{11}}$	γ	θ
$K_{10}Cs_{90}$	798.0	9.037	0.957	1.10	0.595	0	1.032
$K_{20}Cs_{80}$	767.4	9.084	0.889	1.10	0.596	0	1.035
$K_{30}Cs_{70}$	738.0	9.126	0.827	1.10	0.596	0	1.035
$K_{40}Cs_{60}$	713.6	9.161	0.778	1.09	0.592	−0.01	1.026
$K_{50}Cs_{50}$	694.8	9.192	0.742	1.09	0.592	−0.01	1.026
$K_{60}Cs_{40}$	666.5	9.243	0.689	1.09	0.591	−0.005	1.028
$K_{70}Cs_{30}$	624.6	9.305	0.617	1.09	0.586	−0.005	1.022
$K_{80}Cs_{20}$	595.7	9.330	0.570	1.09	0.581	−0.005	1.018
$K_{90}Cs_{10}$	566.7	9.386	0.525	1.09	0.576	0	1.017

Earlier theoretical studies were performed on K-Cs with the integral equation method, but their aim was essentially to ascertain the closure relation used.[6–8] Gopala Rao and Das Gupta[9] also used the integral equation method to study the behavior of this alloy as a function of concentration. However, the interactions were described by square well potentials, which, admittedly, represent a crude approximation for metals. Even if the integral equation method allows to get the low-q behavior of the structural properties, which contains interesting information about chemical order for instance, these results always suffer from the approximation inherent to the closure relation. K-Cs is also one of the few systems, which dynamic structure factor has been measured experimentally by inelastic neutron scattering,[10] but for one composition only. Its dynamic structure was also computed by MD in order to highlight fast sound phenomenon.[11]

In the present work, nine compositions spread at 10 at. % over the entire phase diagram of liquid K-Cs are investigated using large scale classical MD simulations and pair interaction potentials obtained from Fiolhais' pseudopotential within the second-order perturbation method. In a recent set of papers,[12–14] we were interested in the study of the transferability from the solid to the liquid state of a pseudopotential developed by Fiolhais *et al.*[15] This approach was successfully extended to alloys in the case of alkali metals,[16] but was restricted to given compositions. Here, the validity of the interaction model is ascertained by comparing experimental and simulated total structure factors of liquid K-Cs system in the whole concentration range. The low-q limits of the structure factors carrying information about chemical order are usually left out because of insufficient data produced by the simulations. Because of the large size of the simulation boxes considered here, we are able to compute very accurately the partial and total structure factors from the partial pair distribution functions even for small-q values. This enables us to pay attention to the low-q limits of these functions, which are related to the thermodynamic properties of the system. Among them, the isothermal compressibility, χ_T, is obtained as a function of concentration. Concerning the dynamical properties, we study the self- and interdiffusion properties in order to highlight their variation with composition.

This paper is organized as follows. After this introduction, Sec. II will be devoted to the presentation of the theoretical approach, including the description of the interactions, the MD simulations, and the processing of the configurations they produced. In Sec. III, we will display the results for the structural, thermodynamic, and diffusion properties, which will be discussed simultaneously. Finally, we will summarize and conclude in Sec. IV.

II. FORMALISM

Liquid K-Cs alloy is studied for nine different compositions, ranging from 10 to 90 atomic percents of potassium. According to available experimental data, the selected temperature is 373 K and the density is deduced from experiment.[4] Atomic volumes are summarized in Table I. In this paper, subscripts 1 and 2 will refer to potassium and cesium, respectively.

A. Model of interactions

As mentioned above, K-Cs is a nearly free-electron-like metal. Therefore, we use the well-established second-order perturbation determination of the effective pair potentials, $u_{ij}(r)$, which can be written as (in atomic units $e=\hbar=m_e=a_0=2$ Rydberg$=1$)

$$u_{ij}(r) = \frac{Z_i Z_j}{r}\left(1 - \frac{2}{\pi}\int_0^\infty F_{N_{ij}}(q)\frac{\sin qr}{q}dq\right), \tag{1}$$

where

$$F_{N_{ij}}(q) = \left(\frac{q^2}{4\pi}\right)^2 \frac{1}{Z_i Z_j} w_i(q) w_j(q)\left(1 - \frac{1}{\varepsilon(q)}\right)[1 - G(q)], \tag{2}$$

with

$$\varepsilon(q) = 1 - [1 - G(q)][1 - \varepsilon_H(q)]. \tag{3}$$

In these expressions, Z_i denotes the valence of the ions of the ith species. The Lindhardt-Hartree dielectric function

$$\varepsilon_H(q) = 1 + \frac{1}{2\pi k_F \eta^2}\left(\frac{1-\eta^2}{2\eta}\ln\left|\frac{1+\eta}{1-\eta}\right| + 1\right), \quad (4)$$

where $\eta = q/2k_F$ accounts for the electrostatic interactions in the electron gas. The choice of the expressions of both local field correction, $G(q)$, which describes exchange and correlation effects between conduction electrons, and pseudopotential form factor, $w_i(q)$, describing electron-ion interaction, is crucial in order to get reliable interionic forces. This is all the more true in the case of alloys since the environment of an atom changes significantly with the concentration (see for instance the variation of Ω_0 in Table I). According to former studies, we use the Ichimaru and Utsumi[17] expression of the local field correction to account for exchange and correlation effects between electrons. The electron-ion interaction is described by Fiolhais' model of potential[15]

$$w_i(q) = 4\pi Z_i R_i^2 \frac{N}{V} \quad (5)$$

$$\times\left(-\frac{1}{(qR_i)^2} + \frac{1}{(qR_i)^2+\alpha_i^2} + \frac{2\alpha_i\beta_i}{[(qR_i)^2+\alpha_i^2]^2} + \frac{2A_i}{[(qR_i)^2+1]^2}\right), \quad (6)$$

where R_i, α_i, β_i, and A_i denote the parameters of the potential tabulated by the authors (individual values are used). Indeed, we have shown that this combination gives an excellent description of the interactions in pure liquid alkali metals[13,14] and promising results in the case of some of their alloys.[16] Its ability to deal with the mixtures of interest in this work will be discussed by comparing experimental results of the static structure with predictions of MD simulations.

B. Molecular dynamics simulations

Two kinds of classical MD simulations were performed in this study. Indeed, static structural properties must be known in a wide spatial range in order to improve the Fourier transform while interdiffusion, which is a collective dynamic property, requires longer run in order to improve the statistical accuracy.

Consequently, for the study of the static structure, we performed simulations in the microcanonical *NVE*. Verlet's algorithm in the velocity form was used to integrate the equations of motion with a typical time step $\Delta t = 5\times10^{-16}$ s. The N pointlike particles were placed in a cubic box subject to standard periodic boundary conditions and which volume V was determined to reproduce the experimental number density $\rho = N/V$. The interactions were truncated between 2.5 and 3 times the first minimum position of K-K pair potential. At this range, they are much weaker than in the first neighbor's range and no relevant differences were observed by comparison to results obtained with larger cutoff radii. The computations were performed on a parallel computer and each of them required about 500 hours of CPU time of an IBM SP2. Details concerning the parallel algorithm are reported in previous papers.[16,18] In the case of an alloy, it is necessary to take into account not only local topological relaxations, but also chemical short-range order. Since it appears that composition fluctuations are slower than topological ones, we did not only increase the size of the box, but also the simulated time in comparison with pure liquid metals. In order to obtain a sufficient statistical accuracy in the description of the structure factors in the low-q range, we simulated the behavior of 13 500 particles during 250 ps in the production stage. Furthermore, when dealing with mixtures with relatively low concentration in one of the components (namely 10, 20, 80, and 90 at. % of K), the production stage was increased up to 350 ps. The last point specific to alloys to be mentioned is that care must be taken with the thermalization stage. Indeed, it is not sufficient to consider the average of the squared velocities computed over the whole system in order to check the stability of the temperature. K and Cs atoms make up two subsystems with different masses and which must be in thermal equilibrium with each other. The global equilibrium (i.e., determined from all the atoms) is reached one order of magnitude faster than the partial one. Therefore, the thermalization stage had to be extended up to 10 000 time steps (5 ps) in order for the thermal equilibrium to be effective. Independent configurations were sampled each 10 fs from which the partial distribution functions were obtained.

For the reasons mentioned above, diffusion properties were computed from specific simulation runs. These were performed with $N=2048$ particles in the canonical *NVT* ensemble in order to prevent the system from any temperature drift during much longer runs, considering that diffusion properties are very sensitive to the temperature. This also allowed us to increase the time step up to 1 fs. The temperature was controlled using a Nose-Hoover thermostat and, after the thermalization stage (10 ps), the velocities of the particles were stored each femtosecond during 5 ns. The diffusion properties were computed afterwards from these data.

C. Structural and thermodynamic properties

The simulations provided us with topological configurations from which the partial pair distribution functions were obtained. In this work, we computed the Ashcroft-Langreth structure factors[19] that are related to the pair distribution functions, $g_{ij}(r)$, by

$$S_{ij}(q) = \delta_{ij} + \sqrt{c_i c_j}\rho\int_0^\infty [g_{ij}(r)-1]\frac{\sin qr}{qr}4\pi r^2 dr, \quad (7)$$

where c_i is the concentration of the ith species. From the knowledge of these $S_{ij}(q)$, we are able to reconstruct the total structure factors as measured by x-ray or neutron diffusion experiments. These total structure factors can be compared with corresponding experimental results and write

$$S(q) = \frac{c_1 f_1^2 S_{11}(q) + 2\sqrt{c_1 c_2} f_1 f_2 S_{12}(q) + c_2 f_2^2 S_{22}(q)}{c_1 f_1^2 + c_2 f_2^2}, \quad (8)$$

with f_i corresponding to the form factor describing the diffusion of an incident particle by an atom of type i.

We also computed the Bhathia-Thornton's partial structure factors,[20] which can be expressed as

$$S_{\mathrm{NN}}(q) = c_1 S_{11}(q) + c_2 S_{22}(q) + 2\sqrt{c_1 c_2} S_{12}(q), \tag{9}$$

$$S_{\mathrm{NC}}(q) = c_1 c_2 \left(S_{11}(q) - S_{22}(q) + \frac{c_2 - c_1}{\sqrt{c_1 c_2}} S_{12}(q) \right), \tag{10}$$

$$S_{\mathrm{CC}}(q) = c_1 c_2 [c_2 S_{11}(q) + c_1 S_{22}(q) - 2\sqrt{c_1 c_2} S_{12}(q)]. \tag{11}$$

As will be discussed later, they carry information about the order in the mixture on both topological and chemical point of view. Moreover, their low-q limit is related to some thermodynamic properties of the system, namely

$$S_{\mathrm{CC}}(0) = N k_B T \Big/ \left(\frac{\partial^2 G}{\partial c^2} \right)_{T,P,N}, \tag{12}$$

$$S_{\mathrm{NN}}(0) = \frac{N}{V} k_B T \chi_T + \delta^2 S_{\mathrm{CC}}(0), \tag{13}$$

$$S_{\mathrm{NC}}(0) = -\delta S_{\mathrm{CC}}(0), \tag{14}$$

where G is the Gibbs free energy, χ_T is the isothermal compressibility, and δ is a dilatation factor defined as

$$\delta = \frac{N}{V}(v_1 - v_2), \tag{15}$$

with v_i denoting the partial molar volumes of the ith species.

D. Diffusion properties

In a mixture, two different diffusion mechanisms must be distinguished.

The first one is the self-diffusion that is also present in pure liquids. It is an individual property related to the ability of each atom to move into the system. In order to characterize this ability, the self-diffusion coefficient, D_i, of atoms of species i is introduced. It can be obtained from the mean-square displacement, but we computed it from the velocity autocorrelation function (VACF)

$$\psi(t) = \frac{1}{N} \lim_{\tau \to \infty} \frac{1}{\tau} \int_0^\tau \sum_{i=1}^{N} \mathbf{v}_i(t_0) \cdot \mathbf{v}_i(t_0 + t) dt_0, \tag{16}$$

since

$$D = \frac{1}{6} \int_{-\infty}^{+\infty} \psi(t) dt. \tag{17}$$

As in pure liquid metals, $\psi(t)$ carries information about the nature of the movement of the particles, which can also be conveniently displayed by considering the spectral density of the VACF,

$$\tilde{\psi}(\omega) = \int_{-\infty}^{+\infty} \psi(t) \exp(-i\omega t) dt. \tag{18}$$

The low-frequency limit of the spectral density reflects the diffusion properties since $D = \tilde{\psi}(\omega = 0)/6$, while peaks at finite frequencies are related to atomic vibrations.

The second diffusion mechanism to be considered in a mixture is the interdiffusion. This collective property is related to the ability of both chemical species to mix or separate, and is characterized by the interdiffusion coefficient, $D_{\mathrm{K/Cs}}$, introduced in Fick's law. This coefficient can be obtained from simulations of the system at equilibrium[21]

$$D_{\mathrm{K/Cs}} = \frac{c_1 c_2}{S_{\mathrm{CC}}(0)} \int_0^\infty V_D(t) dt, \tag{19}$$

where

$$V_D(t) = \frac{1}{3 N c_1 c_2} \lim_{\tau \to \infty} \frac{1}{\tau} \int_0^\tau \mathbf{v_d}(t_0) \cdot \mathbf{v_d}(t_0 + t) dt_0 \tag{20}$$

is the autocorrelation function of the microscopic diffusion velocity

$$\mathbf{v_d}(t) = c_2 \sum_{i=1}^{N_1} \mathbf{v_i}(t) - c_1 \sum_{j=1}^{N_2} \mathbf{v_j}(t). \tag{21}$$

If the correlations between the velocities of different particles are negligible, the correlation function $V_D(t)$ can be reduced so that

$$D_0 = \int_0^\infty V_D(t) dt = c_{\mathrm{Cs}} D_{\mathrm{K}} + c_{\mathrm{K}} D_{\mathrm{Cs}}. \tag{22}$$

This would not be the case in a molten salt because of Coulomb interactions. Moreover, in an ideal mixture, the interdiffusion coefficient writes

$$D_{\mathrm{K/Cs}} = D_{\mathrm{id}} = c_{\mathrm{Cs}} D_{\mathrm{K}} + c_{\mathrm{K}} D_{\mathrm{Cs}}, \tag{23}$$

since $S_{\mathrm{CC}}(0) = c_{\mathrm{K}} c_{\mathrm{Cs}}$ in such a perfect system.

III. RESULTS AND DISCUSSION

After examining the effective interactions between atoms in the mixtures under consideration, we will display and discuss their static structure. The chemical order will be discussed by considering $g_{ij}(r)$, then $S_{ij}(q)$. The total structure factors will be considered with respect to experiments in order to test the accuracy of the approach. The Bhatia-Thornton structure factors will shed some more light on chemical order, and particular attention will be paid to their low-q limit from which thermodynamic properties will be inferred. In a last part, we will examine our results for the diffusion properties.

A. Pair interactions

Since the structural properties of a system result from the interatomic interactions, let us first examine the pair potentials and their evolution with concentration. In order not to overload the presentation, we do not display figures of $u_{ij}(r)$, but we only summarize some of their main features in Table I, namely σ_{ij} and ϵ_{ij}, which denote the position and the depth of their first minimum, respectively. Indeed, the pair potentials of all these systems have the usual shape of metallic

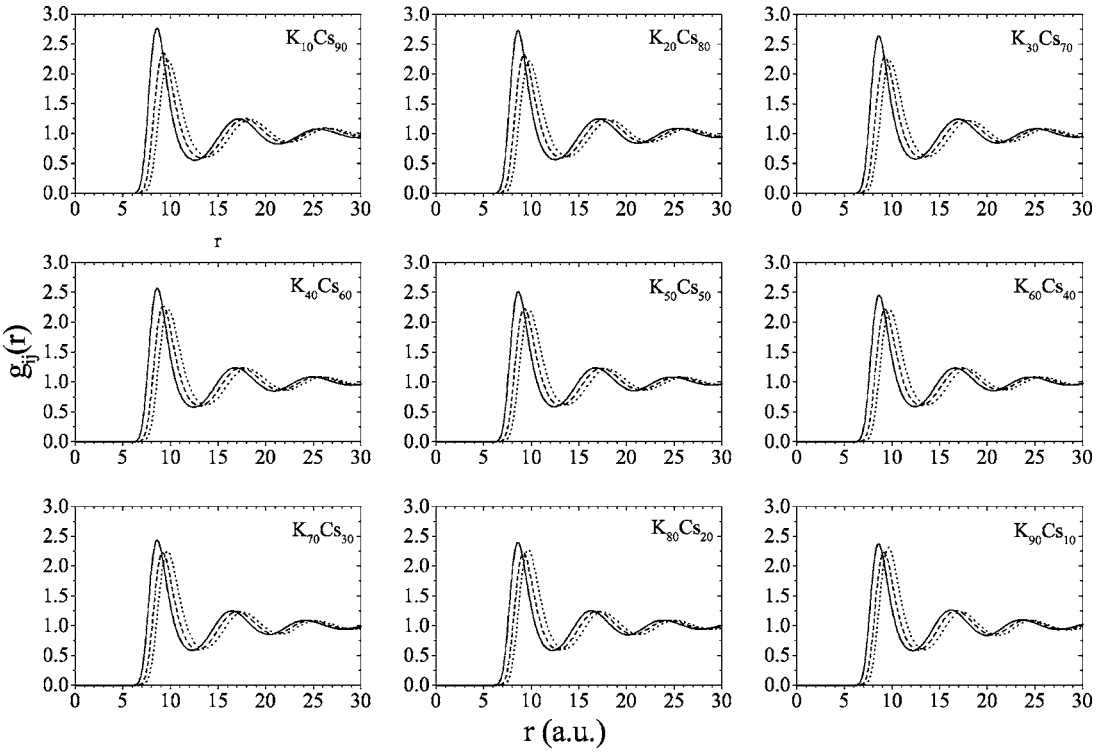

FIG. 1. Partial pair distribution functions for the nine alloys under consideration. Solid, dashed, and dotted lines represent K-K, K-Cs, and Cs-Cs functions, respectively.

effective potentials, namely a short-range repulsive part, followed by a first negative minimum, and long-range Friedel oscillations.

From the essential characteristics of the pair potentials gathered in Table I for each composition, some interesting features of the system can be deduced as, for instance, its departure from ideal and additive mixtures. Strictly speaking, an ideal mixture corresponds to the condition $u_{11}(r)=u_{12}(r)=u_{22}(r)$. In order to characterize the deviation from this situation, we consider the following two ratios: $\alpha=\sigma_{22}/\sigma_{11}$ and $\beta=\epsilon_{22}/\epsilon_{11}$. The first one accounts for size mismatch and the second one for attraction asymmetry. These asymmetries are rather constant versus concentration. Moreover, compared with other mixtures, the absolute values of α and β are rather close to unity, suggesting a weak departure from ideal mixture.

Of course, ideal mixtures are utopian and a more realistic model is the so-called additive mixture. In order to characterize the deviation from this reference model, we consider, in Table I, two other ratios, γ and θ, defined by $\sigma_{12}=(1+\gamma)(\sigma_{11}+\sigma_{22})/2$ and $\epsilon_{12}=\theta\sqrt{\epsilon_{11}\epsilon_{22}}$, the additive case corresponding to $\gamma=0$ and $\theta=1$. It is seen that the interactions in K-Cs are additive as far as the size of the particles is concerned. Considering the attraction between atoms, there is a slight deviation from the additive limit. Anyway, the values of θ remain rather low in comparison with what is observed in Na-Cs for instance ($\theta=1.363$ for $Na_{80}Cs_{20}$ with the same pseudopotential).

A first point to remind is that size asymmetry alone ($\alpha\neq 1$) induces heterocoordination tendencies, as can be established by entropic considerations.[22] Second, following a study carried out by Osman and Singh[23] on Lennard-Jones mixtures with a thermodynamic perturbation approach, attraction asymmetry ($\beta\neq 1$) induces homocoordination, while attraction nonadditivity induces homocoordination if $\theta<1$ and heterocoordination if $\theta>1$. Consequently, there are competing effects in the case of K-Cs. Size asymmetry and attraction nonadditivity induce heterocoordination, while attraction asymmetry is in favor of homocoordination.

Let us now examine the impact of these two features that we have deduced from the interactions directly on the resulting structural properties. As we will see, both tendencies cancel quite completely and this explains why, in a sense, K-Cs behaves nearly like an ideal mixture.

B. Static structure

Although it represents a large amount of data, we have chosen to present the results obtained for each of the nine compositions. To our knowledge, this kind of systematic presentation is lacking in the literature (at least for molecular dynamics results for realistic interaction models) and we believe that it will enable a better understanding of the evolution of the partial structure functions versus composition.

1. Partial pair distribution functions

In Fig. 1, we display the partial pair distribution functions. Partial functions behave in the same way as the total one of pure liquids. Their low- and large-distance limiting values are the result of an exclusion volume due to impenetrability of atomic cores and of the disorder at long distances, respectively. The peaks and minimum are related to the most

TABLE II. Partial coordination numbers and local mole fraction parameter of the alloys under study.

Alloy	n_{11}	n_{12}	n_{21}	n_{22}	x_s-1
$K_{10}Cs_{90}$	1.10	11.18	1.24	11.81	−0.0054
$K_{20}Cs_{80}$	2.26	10.10	2.53	10.62	−0.0095
$K_{30}Cs_{70}$	3.40	9.09	3.90	9.55	−0.0177
$K_{40}Cs_{60}$	4.65	7.99	5.32	8.48	−0.0176
$K_{50}Cs_{50}$	5.86	6.88	6.88	7.17	−0.0297
$K_{60}Cs_{40}$	7.18	5.54	8.31	5.76	−0.0261
$K_{70}Cs_{30}$	8.75	4.41	10.30	4.54	−0.0292
$K_{80}Cs_{20}$	10.09	3.06	12.25	3.12	−0.0297
$K_{90}Cs_{10}$	11.71	1.58	14.20	1.60	−0.0176

(respectively, less) probable distances between neighbors.

In the case of mixtures, additional information is available by comparing partial functions with each other. First, the positions of the first peaks are related to the size of the atoms. The K-Cs first peak lies right in the middle between K-K and Cs-Cs first peaks. This can be related to the above-mentioned size-additivity of the interactions. Second, the heights of the first peaks may exhibit the signature of chemical order. Indeed, if the first peak of $g_{K-Cs}(r)$ was much higher than both others, it would be the signature of heterocoordination tendencies like compound forming. On the other hand, if it were significantly lower than both others, it would reveal homocoordination tendencies. In the case of K-Cs system, no such marked behavior is observed.

We can point out the slight decrease of the K-Cs first peak that becomes lower than the Cs-Cs one in the range $c_K \geqslant 70$ at. %. Preliminary calculations show a similar behavior of the Na-K system and in a more marked extent of Na-Cs in the same concentration range of the lighter element. Strong anomalies of some physical properties of Na-Cs in this range have been related to probable concentration fluctuations in the mixture,[24] and the quest for similar behavior in liquid Na-K alloy has also been questioned[25] in the same range. A last point to be mentioned is the evolution of each $g_{ij}(r)$ versus composition. The partial pair distribution functions are rather insensitive to the concentration of each species. Only slight changes in the height of the first peaks or in their positions can be observed, especially in the low concentration ranges.

In order to get a quantitative measure of the chemical order, we consider the coordination numbers (Table II) defined as

$$n_{ij} = 4\pi \frac{Nc_j}{V} \int_0^{R_{ij}} g_{ij}(r) r^2 dr. \tag{24}$$

It is well known that these quantities suffer for some arbitrariness in the definition of the upper limit of the integral. [R_{ij} is chosen as the position of the first minimum of the corresponding $g_{ij}(r)$.] This is important in the case of alloys since four coordination numbers can be defined according to the chemical nature of the pairs. Direct comparison between partial coordination numbers must be drawn carefully since the volumes considered in counting neighboring atoms depend on the kind of the pairs considered. For instance, neighbors of a K atom are not counted in the same volume if they are K atoms or Cs ones since $R_{KK} \neq R_{KCs}$. Anyway, the difference between these volumes is not too large in the case of K-Cs, weakening this effect.

Coordination numbers are strongly influenced by the concentration of the mixture and chemical order does not always appear clearly. Therefore, various parameters have been proposed in the literature to allow a quantitative description of the chemical order in a mixture. We have chosen the local mole fraction method (see Ref. 26 and references therein)

$$x_s - 1 = \frac{n_{11}}{n_{11}+n_{12}} + \frac{n_{22}}{n_{22}+n_{21}} - 1 \tag{25}$$

since it is independent of the concentration. If the system exhibits complete chemical disorder, $x_s-1=0$, while it becomes positive with homocoordination (it tends to 1 when both components are immiscible) and becomes negative with heterocoordination and compound forming. As can be seen from the values compiled in Table II, x_s-1 is very close to zero, whatever the concentration of the alloy. The values are slightly negative, indicating slight tendency toward heterocoordination. As a comparison, the values obtained in the case of Li-Na alloy[26] in which homocoordination is marked since it exhibits a miscibility gap are about 0.25 above the critical temperature.

Finally, from the evolution of $g_{ij}(r)$ and the values of n_{ij}, we believe that the values obtained for K-Cs can be considered as indications of the absence of chemical order. Consequently, K-Cs behaves rather like a random alloy.

2. Ashcroft-Langreth partial structure factors

According to the large sizes of the boxes and to the lengths of the simulations, $g_{ij}(r)$ curves are smooth enough and their spatial extension is sufficient to compute directly the partial structure factors by Fourier transform without having recourse to any fitting, smoothing or other corrections. This is an important point since any modification of the long-range behavior of $g_{ij}(r)$ may affect the low-q behavior of the structure factors. Moreover, computing directly the structure factors from the configurations for each q value compatible with the box size appears to be of comparable accuracy, but is more time consuming.

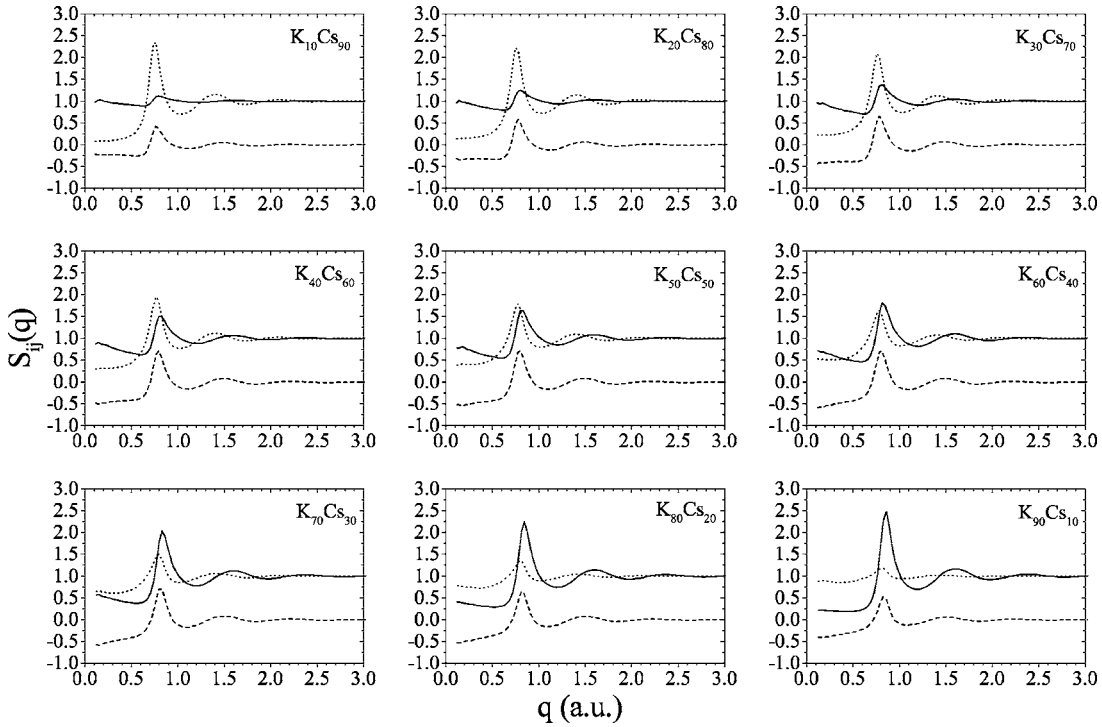

FIG. 2. The Ashcroft-Langreth partial structure factors for the nine alloys under consideration. Solid, dashed, and dotted lines represent K-K, K-Cs, and Cs-Cs functions, respectively.

In Fig. 2, we present the Ashcroft-Langreth partial structure factors. We can underline the smooth behavior of the curves in the low-q limit. Some usual features are recovered, namely $S_{KK}(q)$ and $S_{CsCs}(q)$ oscillate around 1 as q tends to infinity, while $S_{KCs}(q)$ oscillates around 0 in the same limit. The curves are very sensitive to the composition. When varying the concentration, $S_{KK}(q)$ and $S_{CsCs}(q)$ change symmetrically; as the concentration in the corresponding element increases from 10 to 90 at. %, the function goes from a rather flat curve around a constant value equal to 1 even in the small-q range, to a curve looking like the one of a dense pure fluid, exhibiting sharp peaks corresponding to a pronounced structure and low-q values close to 0, but still positive. In the case of K-Cs, it is interesting to notice the nearly symmetrical evolution of these two functions versus concentration. This is again an indication of the quite ideal behavior of the mixture. As for $S_{KCs}(q)$, its changes versus concentration are smaller, except in the low-q range where the limiting values do not vary symmetrically. We shall point out that the negative values of $S_{KCs}(q)$ observed as q tends to 0 are a consequence of the definition of the Ashcroft-Langreth partial structure factors.

In addition, we could also have considered the Faber-Ziman's structure factors,[27] which are sometimes preferred. One method[28] proposed to circumvent the lack of experimental possibility in determining the partial structure factors is to suppose that the Faber-Ziman structure factors are functions independent on the concentration of both species. Our results (not presented here) indicate that, even in the case of a mixture as simple as K-Cs, such an approximation is unreasonable and that the method is ruled out. Indeed, in the case of K-Cs, we observe that they are quite independent on composition only for q values beyond the first minimum.

Not much more can be said about the Ashcroft-Langreth structure factors. Their main interest is that, if they can be extracted from experimental total structure factors, they allow getting a measure of the partial pair distribution functions. In our numerical approach, we proceed in the opposite sense, since we compute the total structure factors from these partial ones in order to compare them with experimental determinations in order to have an estimation of the reliability of our simulations.

3. Total structure factors

As mentioned in the introduction, there are rather few experimental data available for the structure of K-Cs.[2,3] In Fig. 3, we have plotted the total structure factors reconstructed for both neutron and x-ray scattering experiments according to Eq. (8) for the nine compositions under study. These results are compared with corresponding experimental data extracted from the literature curves when available. Whatever the kind of diffusing particle considered or the composition of the mixture, a good agreement is found between simulation and experimental results. Considering the accuracy of the available experimental data, it confirms that the description of the interactions is realistic at the level of the structural properties.

It can also be noticed that there are rather little differences between x-ray and neutron structure factors, especially for low concentrations in K. The differences become noticeable for more than 50 at. % of K. This illustrates the great difficulty encountered in exploiting different sources of measurements to extract partial structures. Even if three independent total structure factors were available, a strong contrast as

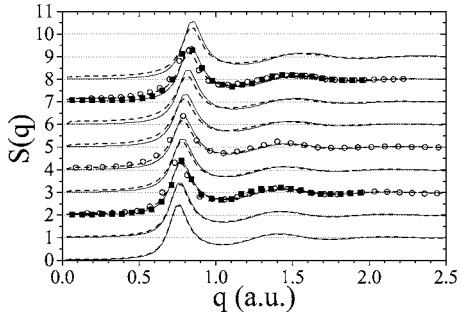

FIG. 3. Total structure factors recomposed for x-ray (dashed curve) and neutron (solid curve) scattering for the nine alloys under consideration and compared with experiment (neutron, full symbols; x ray, open symbols) when available (Refs. 2 and 3). Curves are shifted one unit vertically each time c_K increases 10%.

well as a good accuracy would be necessary to be able to extract accurate partial structure factors in order to deduce partial pair distribution functions. On the other hand, the present study illustrates that numerical simulations can afford an accurate description of the partial structures if the model of interactions is reliable, which is the case here.

4. Bhathia-Thornton partial structure factors

In Fig. 4, we have plotted the Bhathia-Thornton partial structure factors for the nine compositions under consideration. The discussion of the low-q behaviors will be easier when dealing with these functions, which are tailored to describe thermodynamic properties (see Sec. II C). The curves present usual features of the corresponding functions. $S_{NN}(q)$ is related to the topological order between atoms, irrespective of their chemical nature and, therefore, it resembles the structure factor of a pure liquid. As the concentration of Cs is increased, the position of the first peak shifts monotonously from its position in the case of pure potassium to that in the case of pure liquid cesium. The changes of this function with concentration are rather small, and, consequently, it appears that topological order is quite insensitive to the chemical composition, suggesting a substitution alloy. As the composition of the mixture is changed, atoms of one kind replace atoms of the other one site for site. $S_{NC}(q)$ oscillates around zero. Its oscillations are the largest in the equiatomic mixture and decrease as species become predominant. $S_{CC}(q)$ is related to the chemical order since it corresponds to the correlations between concentration fluctuations. In the case of an ideal mixture, it is equal to c_1c_2 for all q. In the case of K-Cs, for every composition, the curves are quite constant although fluctuations appear around the ideal value. Anyway, these differences remain very small in comparison with other systems like Na-K or Na-Cs. The behavior of $S_{CC}(q)$ can be related to that of the corresponding intermediate scattering function, $F_{CC}(q,t)$, as observed by Chushak and Baumketner[11] from their results of molecular dynamics simulations for two compositions of the mixture. Indeed, $F_{CC}(q,t)$ is a monotonously decreasing function of time for every q-value considered, indicating the absence of fluctuations of concentration.

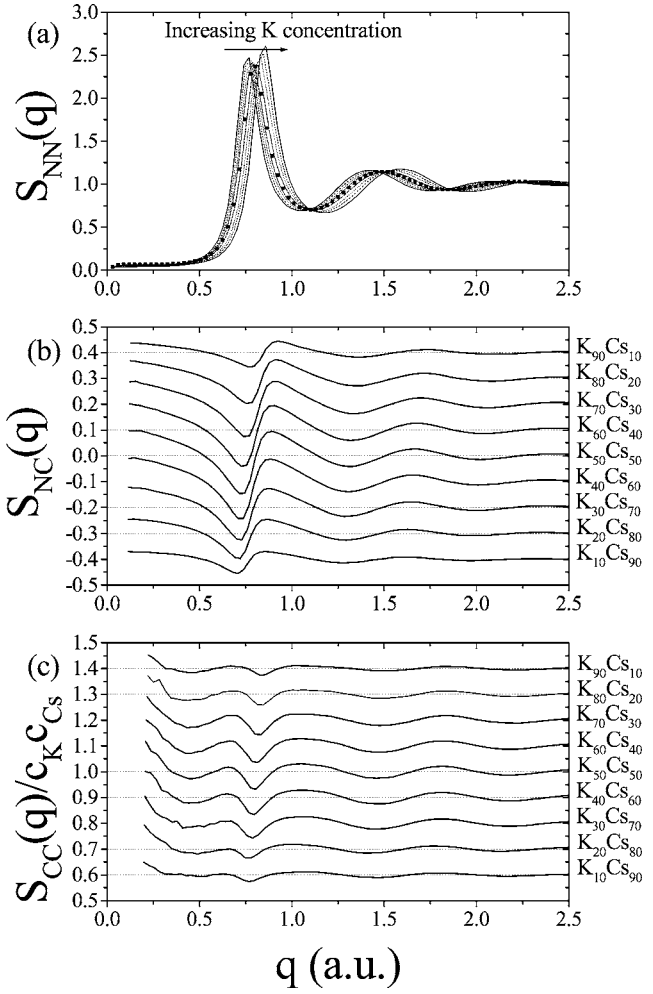

FIG. 4. The Bhatia-Thornton partial structure factors (a) $S_{NN}(q)$, (b) $S_{NC}(q)$, and (c) $S_{CC}(q)/c_Kc_{Cs}$ for the nine alloys under consideration. In (b) and (c), curves are shifted an amount $(c_K-0.5)$ vertically.

C. Thermodynamic properties

The large scale of the simulations performed allows us to examine also the low-q limit of the structure factors. Indeed, the large size of the simulation boxes allows us to perform a fine sampling of the structure factors. Moreover, the long simulated times guarantee a high statistical accuracy down to q values very close to 0. In fact, only 4 or 5 of the first points in the range $0 \leqslant q \leqslant 0.15$ a.u.$^{-1}$ of the structure factors are spoiled by statistical noise and removed from the curves displayed in this work. We also believe that this must be done due to the cutoff radius of the interactions. As mentioned in Sec. II C, one of the main interests of the Bhatia-Thornton structure factors lies in their low-q limit, which are related to thermodynamic quantities. Consequently, we can extrapolate the curves in order to obtain estimations of the $q=0$ values of the structure factors and of the related thermodynamic quantities. For this purpose, we have interpolated the curve in the low-q range by suitable functions, namely a second order polynomial for $S_{CC}(q)$, and the expression $A+B\exp[(q-C)/D]$ for $S_{NN}(q)$ and $S_{NC}(q)$. These functions interpolate accurately the corresponding data and do not behave spuriously out of the considered interval.

TABLE III. Extrapolated low-q limits of the Bhatia-Thornton partial structure factors and deduced dilatation factor, δ_{DM}, and isothermal compressibility, χ_T. The experimental value, δ_{expt}, is computed from the density measurements (Ref. 4).

Alloy	$S_{NN}(0)$	$S_{NC}(0)$	$S_{CC}(0)$	σ_{expt}	δ_{DM}	χ_T (10^{-10} Pa^{-1})
$K_{10}Cs_{90}$	0.037	0.031	0.10	−0.370	−0.310	6.28
$K_{20}Cs_{80}$	0.047	0.060	0.18	−0.384	−0.333	5.96
$K_{30}Cs_{70}$	0.052	0.083	0.24	−0.400	−0.346	4.95
$K_{40}Cs_{60}$	0.058	0.100	0.28	−0.413	−0.357	4.58
$K_{50}Cs_{50}$	0.062	0.110	0.30	−0.425	−0.367	4.32
$K_{60}Cs_{40}$	0.061	0.110	0.30	−0.442	−0.367	3.96
$K_{70}Cs_{30}$	0.056	0.097	0.26	−0.472	−0.373	3.56
$K_{80}Cs_{20}$	0.050	0.074	0.19	−0.492	−0.389	3.63
$K_{90}Cs_{10}$	0.040	0.042	0.10	−0.521	−0.420	3.64

The values obtained are displayed in Table III. They are smooth functions of concentration, which is an indication of the quality of the results that are not blurred by statistical noise. Although the absolute accuracy of these values can be questioned, they provide some information about the qualitative behavior of the system. First of all, $S_{CC}(0)$ is slightly greater than c_1c_2 for the nine compositions studied. As is well known, this is the sign of a slight tendency towards homocoordination and confirms the conclusion we were led to concerning the partial distribution functions and structure factors. As we can see, these different clues indicate that, within the accuracy of the calculations, K-Cs can be considered as an ideal system on the chemical order point of view.

Second, we can also use the extrapolated values in order to estimate some thermodynamic properties. The first one is δ introduced by relation (14). It is defined as a ratio between the partial molar volumes of the constituents of the mixture and can be deduced from the knowledge of the density of the system that was measured experimentally.[4] Since the density of K-Cs is linear versus concentration within the experimental accuracy, the determination of an experimental value of δ is straightforward, which can be compared with the one obtained from the ratio $S_{NC}(0)/S_{CC}(0)$. In Table III, it can be observed that the simulation results, δ_{DM}, underestimate the experimental value, δ_{expt}, of about 15%, but the variation versus composition is correct. Nevertheless, the differences are compatible with the accuracy of density data. Indeed, if we suppose a parabolic dependence of density with concentration, δ_{expt} changes of up to 30%.

The second thermodynamic property of interest is the isothermal compressibility. It can be deduced from relation (13) and from the values of δ. The results are plotted in Fig. 5 with the corresponding experimental values for pure K and Cs (Ref. 29) and values obtained analytically by Gopala Rao and Das Gupta[9] with square well interaction model within the mean spherical approximation. The simulation results display a smooth variation of χ_T versus concentration and the curve is consistent with the experimental values for the pure elements. This is not the case for the analytical model. An interesting point emerging from our results is that the evolution of χ_T as a function of concentration is lower than a linear interpolation between the pure systems values. This could be explained by the following way: since K atoms are smaller than Cs ones, when mixing both kinds of atoms together, potassium tends to occupy interstitial volumes between cesium ones. As a consequence, the mixture is more compact than the mean of the corresponding volumes of the pure elements and its compressibility is lower. One should recover this effect on density, but it remains nevertheless very weak since size asymmetry is low and may not be distinguished from the experimental error.

D. Diffusion properties

Let us first examine the self-diffusion properties. In Fig. 6 are displayed the VACF of both K and Cs atoms for the nine compositions under study. The usual shape of these functions is recovered. After a rapid decrease, they become negative and reach a first minimum, indicating the rebound of the atoms against their neighbors. This is the so-called cage effect. At longer time, the functions oscillate until they reach the zero-asymptotic limit corresponding to a complete loss of correlation. As the composition changes, the environment of the atoms evolves and this is recovered in the VACF features. Indeed, the more there will be cesium atoms in the mixture,

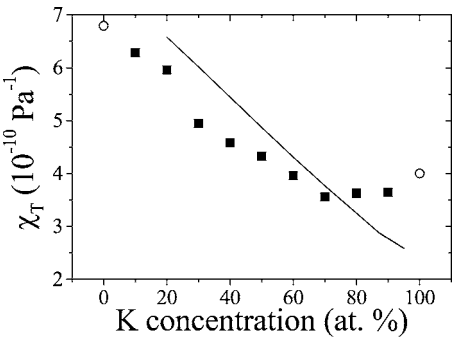

FIG. 5. Isothermal compressibility deduced from the low-q limits of the Bhatia-Thornton partial structure factors (full squares). Experimental values for the corresponding pure elements (open circles) are also reported (Ref. 29), as well as results obtained by Gopala Rao and Das Gupta (Ref. 9) with an analytical model (solid line).

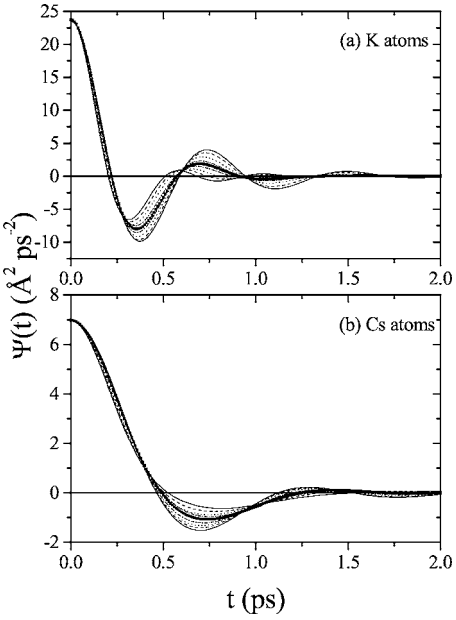

FIG. 6. VACF of (a) K and (b) Cs atoms for the nine systems studied. As c_K decreases, the first minimum of $\psi_K(t)$ and $\psi_{Cs}(t)$ becomes deeper.

the stronger the cage effect will be since cesium atoms are heavier than potassium ones. Consequently, as c_{Cs} increases, the oscillations are getting ampler. Moreover, due to their lighter mass, potassium atoms undergo more important backscattering than cesium ones. For the same reason, the velocity of K atoms is higher, so that the decrease of their VACF is faster and the frequencies of the oscillations higher. These trends are recovered in Fig. 7 where we display the spectral densities of the VACF. In the case of potassium atoms, we can point out that the position of the peak is not very sensitive to the composition, but, as x_{Cs} increases, it becomes sharper, i.e., with a better defined characteristic frequency. This is consistent with an increase of the cage effect, the cage being formed by more and more heavier Cs atoms. On the other hand, the curves for Cs evolve differently. As the concentration of K atoms increases, the oscillating behavior lowers, but the reason is the same. In both cases, the low frequency limit, which is related to the self-diffusion coefficient is not very sensitive to the composition. The corresponding values of D_K and D_{Cs} gathered in Table IV confirm this point. We estimate the statistical uncertainty to about 3% for these values.

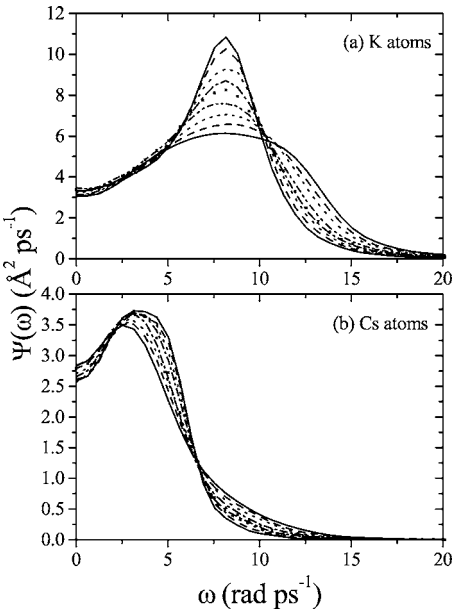

FIG. 7. Spectral density of the VACF of (a) K and (b) Cs atoms for the nine systems studied. As c_K decreases, the height of the peaks of $\tilde{\psi}_K(\omega)$ and $\tilde{\psi}_{Cs}(\omega)$ increases.

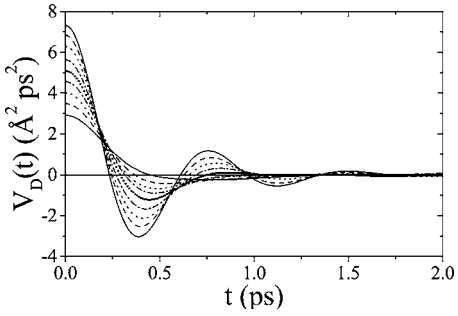

FIG. 8. Autocorrelation functions of the interdiffusion fluxes. As c_K decreases, the $t=0$ value increases.

We now turn to the interdiffusion properties. The autocorrelation functions of the interdiffusion fluxes are displayed in Fig. 8. According to Eq. (22), we can obtain D_0 by integration of these curves. We estimate the statistical accuracy of D_0 to about 5%. Since we performed large scale MD simulations, we know an accurate estimate of $S_{CC}(0)$ (see Table III). This enables us to compute the interdiffusion coefficient, $D_{K/Cs}$, that remains rather constant versus composition as can be seen from the values presented in Table IV although the amplitude of $V_D(t)$ decreases strongly as c_K increases. Some comments can be done. First, the quite constant value of the interdiffusion coefficients, $D_{K/Cs}$, versus composition is specific to K-Cs. For instance, in the case of Ni-Al,[30] it is 2 to 3 times higher in Al-rich alloys than in Ni-rich ones. Second, if we consider D_0, its values agree with D_{id} within statistical accuracy. As mentioned before, this implies a very weak coupling between the velocities of atoms of different species. Third, if we compare our results for the interdiffusion coefficient $D_{K/Cs}$, to the case of the ideal mixture model prediction, D_{id}, we can see that they are always lower than those of this simple model. It is related to the values of $S_{CC}(0)$ that are higher than $c_K c_{Cs}$. This is an interesting point since the ideal mixture assumption is often used for want of anything better. In the case of K-Cs, the incidence exists, but is not too important. This should not be the case for other systems like Na-Cs and numerical simulations should be helpful, at least on a qualitative point of view.

IV. CONCLUSION

In this work, we performed large scale MD simulations of liquid K-Cs alloys as a function of composition. A comparison to available experimental data for the structural proper-

TABLE IV. Self-diffusion and interdiffusion coefficients in $Å^2\ ps^{-1}$. Notations are defined in the text.

Alloy	D_K	D_{Cs}	$D_{K/Cs}$	D_0	D_{id}
$K_{10}Cs_{90}$	0.510	0.431	0.428	0.475	0.503
$K_{20}Cs_{80}$	0.518	0.435	0.435	0.489	0.501
$K_{30}Cs_{70}$	0.512	0.438	0.443	0.507	0.490
$K_{40}Cs_{60}$	0.523	0.454	0.447	0.521	0.496
$K_{50}Cs_{50}$	0.563	0.465	0.460	0.552	0.514
$K_{60}Cs_{40}$	0.575	0.474	0.434	0.543	0.514
$K_{70}Cs_{30}$	0.540	0.457	0.413	0.512	0.492
$K_{80}Cs_{20}$	0.553	0.478	0.433	0.515	0.493
$K_{90}Cs_{10}$	0.550	0.472	0.462	0.513	0.480

ties shows that the description of the interactions is reliable.

The large number of atoms used enabled us to give an accurate description of the structural properties, even in the low-q range. Unlike experiments, simulation gives easily access to partial structure functions. The accuracy of our results in the small-q range allowed us to get information about the thermodynamic properties of the system, which are consistent with available experimental data within the experimental accuracy. We are also able to get information about the diffusion properties. Therefore, MD simulations can valuably play a role, which is complementary to the experimental investigation.

We are enlightened about the behavior of liquid K-Cs alloys. Although this system is not, strictly speaking, an ideal mixture since size asymmetry between both species induces small effects on the topological disorder, it appears to be characterized by a quite complete chemical disorder. It can be seen in the behavior of the partial pair distribution functions, and especially in the chemical order parameter deduced from the partial coordination numbers. It is also apparent in the behavior of the Bhatia-Thornton structure factors. $S_{NN}(q)$ changes only slightly with concentration, indicating that topological order is rather insensitive to the concentration. Moreover, $S_{CC}(q)$ is quite structureless and its low-q limit is very close to the ideal one. Consequently, K-Cs can be considered as a mixture without chemical order and deviations towards homocoordination [as shown by $S_{CC}(0)$] or heterocoordination (as shown by x_s-1) are within the accuracy of the method. In fact, perfect chemical disorder is the boundary between both tendencies and cannot be reached exactly in practice. Therefore, we believe that systems getting close to this behavior are difficult to describe because small changes in the interactions can induce a transformation from one tendency into the other one.

The diffusion properties also exhibit quite an ideal behavior. Self-diffusion coefficients are nearly constant versus composition and the difference between both species is mainly due to the mass difference between K and Cs atoms. Moreover, even the interdiffusion seems unaffected by the composition of the mixture and is really close to the ideal mixture. This is not surprising if we analyze this from the features of the interactions where competing effects appeared between size asymmetry and attraction nonadditivity, on one side, and attraction asymmetry on the other side. This competition results in a quite complete cancellation between homocoordination and heterocoordination tendencies and gives a strong support to the ideal behavior seen in the structure and dynamics properties.

This study offers some interesting prospects. The approach can be extended to other properties like dynamic structure factors, or applied to other alloys. Since K-Cs is a kind of reference system, comparison with other ones will enable to point out their particular behavior. For instance, Na-Cs certainly exhibits more complex evolution versus composition and computations are under way.

ACKNOWLEDGMENTS

The CINES (Centre Informatique National de l'Enseignement Supérieur) is gratefully acknowledged for providing the authors with computer time under Contract No. TMC1928.

*Present address: Laboratoire de Thermodynamique et Physico-Chimie Métallurgique, 1130, rue de la Piscine, Domaine Universitaire, BP 75, 38402 St-Martin d'Hères cedex, France.

[1] J. B. Suck, D. Raoux, P. Chieux, and C. Riekel, *Proceedings of the ILL/ESRF Workshop on Methods in the Determination of Partial Structure Factors of Disordered Matter by Neutron and Anomalous X-Ray Diffraction* (World Scientific, Singapore, 1993).

[2] B. P. Alblas, W. van der Lugt, O. Mensies, and J. T. M. de Hosson, J. Phys. (Paris), Colloq. **41**, C8-153 (1980).

[3] B. P. Alblas, W. van der Lugt, O. Mensies, and C. van Dijk, Physica B & C **106B**, 22 (1981).

[4] P. E. Potter, D. N. Kagan, A. D. Le Claire, and W. van der Lugt, in *Handbook of Thermodynamic and Transport Properties of Alkali Metals*, edited by R. X. Ohse (Blackwell, Oxford, 1985).

[5] P. E. Potter and M. H. Rand, in *Handbook of Thermodynamic and Transport Properties of Alkali Metals*, edited by R. X. Ohse (Blackwell, Oxford, 1985).

[6] G. Kahl, Phys. Rev. A **43**, 822 (1991).

[7] G. Kahl and M. Kristufek, Phys. Rev. E **49**, R3568 (1994).

[8] G. Kahl, B. Bildstein, and Y. Rosenfeld, Phys. Rev. E **54**, 5391 (1996).
[9] R. V. Gopala Rao and B. Das Gupta, Phys. Rev. B **32**, 6429 (1985).
[10] L. E. Bove, F. Sacchetti, C. Petrillo, and B. Dorner, Phys. Rev. Lett. **85**, 5352 (2000).
[11] Y. Chushak and A. Baumketner, Eur. Phys. J. B **7**, 129 (1999).
[12] J. F. Wax, R. Albaki, and J. L. Bretonnet, Phys. Rev. B **62**, 14818 (2000).
[13] J. F. Wax, R. Albaki, and J. L. Bretonnet, Phys. Rev. B **65**, 014301 (2002).
[14] R. Albaki, J. F. Wax, and J. L. Bretonnet, Phys. Rev. B **66**, 014201 (2002).
[15] C. Fiolhais, J. P. Perdew, S. Q. Armster, J. M. MacLaren, and M. Brajczewska, Phys. Rev. B **51**, 14001 (1995); **53**, 13193(E) (1996).
[16] J. F. Wax, N. Jakse, and I. Charpentier, Physica B **337**, 154 (2003).
[17] S. Ichimaru and K. Utsumi, Phys. Rev. B **24**, 7385 (1981).
[18] N. Jakse and I. Charpentier, Mol. Simul. **23**, 293 (2000).
[19] N. W. Ashcroft and D. C. Langreth, Phys. Rev. **155**, 685 (1967).
[20] A. B. Bhatia and D. E. Thornton, Phys. Rev. B **2**, 3004 (1970).
[21] D. B. Boercker and E. L. Pollock, Phys. Rev. A **36**, 1779 (1987).
[22] R. N. Singh and F. Sommer, Rep. Prog. Phys. **60**, 57 (1997).
[23] S. M. Osman and R. N. Singh, Phys. Rev. E **51**, 332 (1995).
[24] M. J. Huijben, T. Lee, W. Reimert, and W. van der Lugt, J. Phys. F: Met. Phys. **7**, L119 (1977).
[25] B. P. Alblas and W. van der Lugt, J. Phys. F: Met. Phys. **10**, 531 (1980).
[26] M. Canales, D. J. Gonzalez, L. E. Gonzalez, and J. A. Padro, Phys. Rev. E **58**, 4747 (1998).
[27] T. E. Faber and J. M. Ziman, Philos. Mag. **11**, 153 (1965).
[28] N. C. Halder and C. N. J. Wagner, J. Chem. Phys. **47**, 4385 (1967).
[29] A. N. Papathanassiou, J. Grammatikakis, and N. Bogris, Phys. Status Solidi A **125**, 529 (1991).
[30] M. Asta, D. Morgan, J. J. Hoyt, B. Sadigh, J. D. Althoff, D. de Fontaine, and S. M. Foiles, Phys. Rev. B **59**, 14271 (1999).